

# RF MEMS Zipping Varactor With High Quality Factor and Very Large Tuning Range

Suan Hui Pu, *Member, IEEE*, David A. Darbyshire, Robert V. Wright, Paul B. Kirby, Mihai D. Rotaru, *Member, IEEE*, Andrew S. Holmes, and Eric M. Yeatman, *Fellow, IEEE*

**Abstract**—An RF MEMS zipping analog varactor with a high-permittivity bismuth zinc niobate dielectric has been fabricated and characterized. The varactor can be continuously tuned from 10 to 280 fF, with a very large tuning range of 2700%. By use of gold electrodes to ensure a low series resistance, the high quality factors of 317 and 63 at 1 GHz were measured for the minimum and maximum capacitances, respectively. The self-resonance frequency of the varactor is estimated to be 16.6 GHz at the maximum capacitance and 87.6 GHz at the minimum capacitance. With a small device footprint of  $540 \times 130 \mu\text{m}^2$ , the zipping varactor is suitable for application in portable reconfigurable RF systems.

**Index Terms**—Radio-frequency microelectromechanical device, microwave device, tunable capacitor, variable capacitor, analog varactor, high-k dielectric, bismuth zinc niobate.

## I. INTRODUCTION

RF ANALOG varactors based on microelectromechanical systems (MEMS) technology offer a number of significant advantages over semiconductor devices, including a high quality factor ( $Q$ -factor), low power consumption, large tuning range and high linearity with respect to RF power [1]. A wide variety of designs for MEMS analog varactors have been reported in the literature and commercially available products are also beginning to emerge. The analog varactors can broadly be categorized as either gap-tuned [2], [3] or area-tuned varactors [4]–[6], where the change in capacitance is achieved by actuating a change in electrode gap or electrode overlap area, respectively.

Zipping varactors are a subset of gap-tuned varactors, where the capacitance change is achieved by the zipping and unzipping action of the two capacitor electrodes using electrostatic actuation [7]–[10]. Zipping varactors are able to achieve very large tuning ranges, high  $Q$ -factors and low power consumption in a very compact form factor. Alternative

Manuscript received July 27, 2016; accepted August 6, 2016. Date of publication August 15, 2016; date of current version September 23, 2016. This work was supported by the EPSRC U.K. under Grant EP/D064805/1 and Grant EP/D064783/1. The review of this letter was arranged by Editor L. K. Nanver.

S. H. Pu and M. D. Rotaru are with the University of Southampton Malaysia Campus, Iskandar Puteri 79200, Johor, Malaysia (e-mail: sp5r11@soton.ac.uk).

D. A. Darbyshire and R. V. Wright were with the Microsystems and Nanotechnology Centre, Cranfield University, Bedfordshire, MK43 0AL, U.K.

P. B. Kirby was with the Microsystems and Nanotechnology Centre, Cranfield University, Bedfordshire, MK43 0AL, U.K. He is now with the Precision Engineering Institute, Cranfield University, Bedfordshire, MK43 0AL, U.K.

A. S. Holmes and E. M. Yeatman are with the Department of Electrical and Electronic Engineering, Imperial College London, London, SW7 2AZ, U.K.

Color versions of one or more of the figures in this letter are available online at <http://ieeexplore.ieee.org>.

Digital Object Identifier 10.1109/LED.2016.2600264

methods of obtaining large tuning ranges include interconnecting either capacitive switches or analog varactors in parallel to achieve multi-bit digital varactors [7], [11], [12], or using large displacement piezoelectric actuators [6], [13], thermal actuators [3], [12] or a rotational comb drive [5]. Digital varactors are very reliable and have good power handling capabilities. However, they require a large device footprint and the cost of integration increases due to the interconnects required. Thermally-actuated varactors are power hungry although the power consumption can be reduced by using latching mechanisms to hold the varactor in various states. Varactors with piezoelectric actuation are power efficient and can achieve large displacements at low voltages (<10 V).

This letter reports a new zipping analog varactor that is able to achieve a very large continuous tuning range (2700%). By using actuation voltages in the range 0 to 30 V, the varactor capacitance can be varied between  $C_{min} = 10 \text{ fF}$  and  $C_{max} = 280 \text{ fF}$ . Using electrostatic actuation, and a tapered cantilever which effectively increases the bending stiffness with increasing width, the pull-in instability is limited to the initial contact and thereafter stable tuning is possible. The varactor has a bismuth zinc niobate (BZN) thin film dielectric with high permittivity, and a large tuning range is achieved in a small device footprint of  $540 \times 130 \mu\text{m}^2$  (including bond pad). Gold varactor electrodes are used in order to keep the series resistance low, resulting in a high  $Q$  at the maximum capacitance (>300 at 8 GHz). This zipping varactor is a significant improvement over an earlier version with  $\text{SiO}_2$  dielectric reported in [10]. By developing a new process that integrates BZN, and improving alignment, the new varactor has smoother tuning characteristics and larger tuning range, demonstrating the potential of zipping varactors.

## II. DESIGN AND FABRICATION

Figure 1 shows a cross-section of the zipping varactor at the symmetric mid-plane. The 300 nm thick BZN dielectric was deposited using RF magnetron sputtering onto a four-inch fused silica wafer which had been coated with 10/200/100 nm of Ti/Au/Pt (bottom actuation electrode). The Pt layer serves as a nucleation layer and diffusion barrier, preventing Au from diffusing into the BZN. Post deposition, the BZN was recrystallized at 350 °C using a combination of hotplate annealing and rapid thermal annealing. The BZN layer had a very high dielectric breakdown strength of 2.0 MV/cm, a low dielectric loss of 0.0015 and a high relative permittivity of 100. A  $\text{CHF}_3/\text{Ar}$  reactive ion etch (RIE) was developed to pattern the BZN with a nickel hard mask [14].

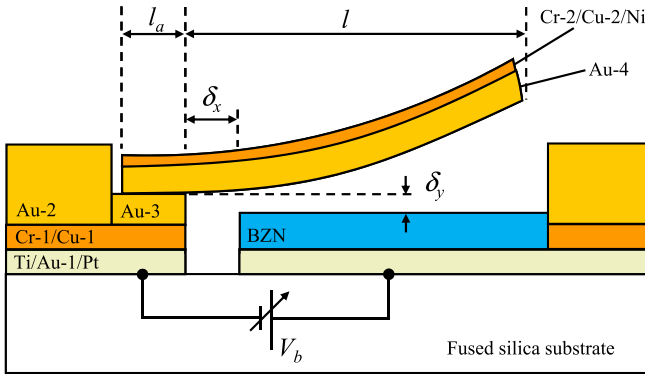


Fig. 1. Varactor cross-section showing device layers and important varactor dimensions.

DC electroplating using a copper seed layer and patterned resist molds was used to deposit the coplanar waveguide (CPW) transmission line ( $2.4 \mu\text{m}$  thick Au-2 layer) and the bond pad (700 nm thick Au-3) in two successive steps. The CPW signal line has a width of  $80 \mu\text{m}$  with gaps of  $10 \mu\text{m}$  between the signal (S) and ground (G) lines. A small gap separates the bottom electrode from the anchor pad ( $\delta_x = 10 \mu\text{m}$ ). The cantilever is connected to the CPW ground through connections between the anchor pad and the ground lines, resulting in a shunt varactor design.

The varactor cantilever (length,  $l = 410 \mu\text{m}$ ) was fabricated on a separate carrier wafer using a process similar to that described in [10]. The Cr-2, Cu-2, Ni and Au-4 layers have thicknesses of 20, 100, 60 and 1170 nm, respectively. Subsequently, the cantilever was attached to the bond pad using a die-level thermosonic bonding process to connect the Au-3/Au-4 interface. The square bond area is defined by the anchor length ( $l_a = 130 \mu\text{m}$ ). After removing the carrier die, the cantilever has a resultant upward curvature due to a stress gradient determined primarily by the tensile, sputter-deposited Cr-2/Cu-2 layers and the relatively stress-free electroplated Au-4 layer. The stress in the Cr-2/Cu-2 layers had a variation within 5% from run to run. Therefore, the repeatability of the process is reasonable even though the current process has not been fine tuned for mass production.

For zero actuation voltage ( $V_b = 0 \text{ V}$ ), the height of the cantilever at the free end is  $70 \mu\text{m}$  and the minimum separation between the bottom of the cantilever and the BZN,  $\delta_y$  is  $0.5 \mu\text{m}$ . Figure 2(a) shows a scanning electron microscopy (SEM) image of the fabricated zipping varactor when no actuation voltage is applied. The width of the cantilever increases linearly from  $20 \mu\text{m}$  at the anchor to  $90 \mu\text{m}$  at the free end. This causes the flexural stiffness of the cantilever to increase progressively along its length, allowing continuous capacitance tuning using electrostatic actuation. The taper in the cantilever is a key feature that enables stable zipping in the varactor without which the device will behave like a capacitive switch. The width of the BZN dielectric is the same as the width of the actuation electrode ( $b_e = 20 \mu\text{m}$ ).

### III. MEASUREMENT RESULTS AND DISCUSSION

The zipping varactor was characterized between 0.1 and 8 GHz using a vector network analyzer (Agilent E8361A).

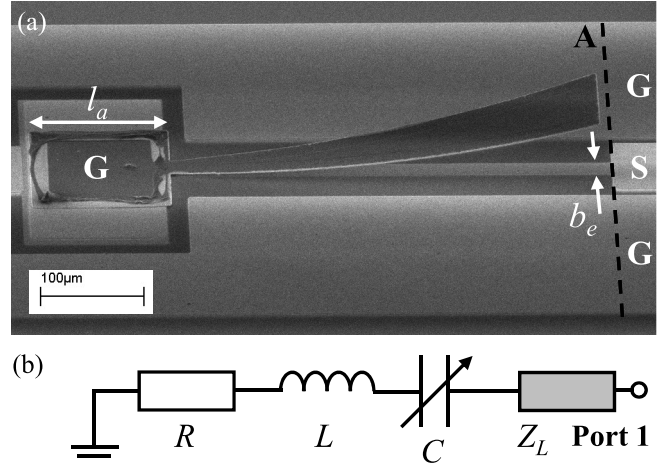


Fig. 2. (a) Scanning electron micrograph of zipping varactor and (b) equivalent circuit model of the varactor and CPW transmission line.

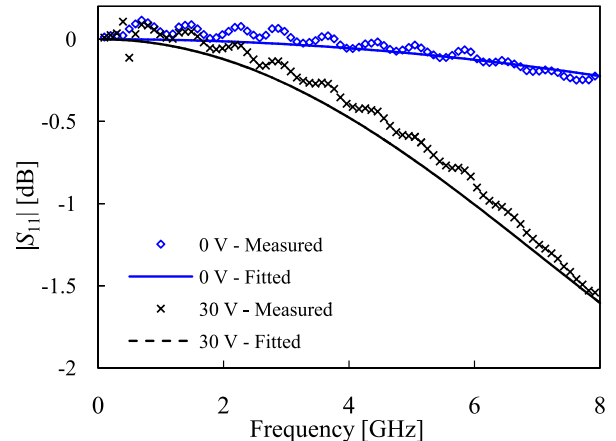


Fig. 3. Measured and fitted varactor  $S_{11}$  magnitudes with 0 V and 30 V actuation voltages applied.

A 2-port short-open-load-through (SOLT) calibration was performed using impedance standard substrates (Cascade Microtech 101-190C) before taking 1-port measurements on the varactor. To tune the varactor, a bias-tee was used to apply a DC bias across the ground and signal tips of the RF probe. The bias voltage was ramped up from 0 to 30 V and then from 30 V down to 0 V. The measured  $S_{11}$  magnitudes at 0 and 30 V are shown in Fig. 3.

An equivalent circuit model, shown in Fig. 2(b), was fitted to the measured  $S_{11}$  in order to extract the varactor capacitance. The varactor is modeled as a variable capacitor  $C$  in series with a resistor ( $R = 0.1 \Omega$ ) and an inductor ( $L = 0.33 \text{ nH}$ ), where the values for  $L$  and  $R$  were determined from the measurements such that the model  $S_{11}$  fits well with the measured  $S_{11}$  across the frequency sweep range at any value of  $V_b$ . The distributed line element  $Z_L$  represents the lossy CPW transmission line between measurement port 1 and plane A, as shown in Fig. 2(a). The measured and fitted  $S_{11}$  magnitudes are shown in Fig. 3 for actuation voltages of 0 and 30 V.

The parameter extracted capacitance,  $C$  of the zipping varactor is shown in Fig. 4. The measured results show a monotonic increase in capacitance from 10 to 280 fF when

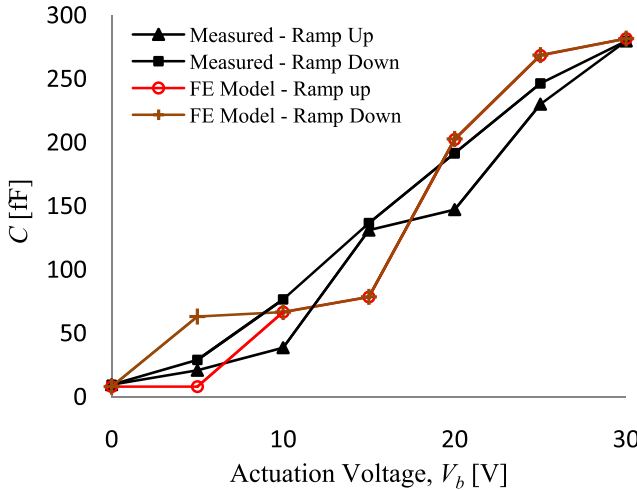


Fig. 4. Measured and simulated capacitance versus tuning voltage showing the trends for both increasing and decreasing actuation voltages.

ramping up the tuning voltage. Similarly, there is also a monotonic decrease in capacitance when the tuning voltage is ramped down to zero. There is some hysteresis in the varactor tuning (at around 15 V and 25 V) due to alignment errors in the bonding of the cantilever. For the same reason, the trend in capacitance increment is not as smooth as the trend in capacitance decrement because some undesired pull-in or sliding between the bottom of the cantilever and the surface of the BZN dielectric can occur during tuning. However, the smooth release of the cantilever from the BZN surface leads to a smooth decrease in capacitance when the actuation voltage is ramped down. For comparison the capacitance of an electromechanical finite element (FE) model is also included in Fig. 4. From the results of the FE model, there is an initial pull-in to close the gap  $\delta_y$  at around 10 V followed by stable zipping up to 30 V due to the tapered design of the cantilever. During ramp down, there is hysteresis below 10 V due to the initial pull-in. The discrepancy between the simulated and measured results is likely due to fabrication process imperfections such as bonding misalignment. In addition, the gap  $\delta_y$  depends on both the height of Au-3 and also the bonding for the current process. For mass production, a monolithic process with a sacrificial layer to determine the thickness of  $\delta_y$  should prove to be more repeatable.

The maximum capacitance of the varactor  $C_{max}$  is much lower compared to an ideal capacitor of the same dimensions assuming perfect contact between the electrodes and the dielectric. For an ideal capacitor with  $400 \times 20 \mu\text{m}^2$  area and a 300 nm thick BZN dielectric, the capacitance value will be 23.6 pF. The measured  $C_{max}$  is 0.28 pF which is much lower due to the imperfect contact of the cantilever with the varactor. Apart from the lengthwise curvature of the cantilever, the beam is also curved in the direction perpendicular to the plane of Fig. 1 (biaxial curvature). Moreover, the roughness average ( $R_a$ ) of the BZN is around 20nm. The biaxial curvature of the cantilever and the roughness of the BZN result in the lower than expected capacitance values.

The  $Q$ -factors of the zipping varactor at 1 GHz are 317 and 63 at  $C_{min}$  and  $C_{max}$ , respectively. The  $Q$ -factors

TABLE I  
COMPARISON OF RF MEMS VARACTORS

Varactor	$C_{min}$ [pF]	$C_{max}$ [pF]	Tuning Range* (%)	$Q$ (GHz)	Actuation Voltages
Borwick [4]	1.4	11.9	750	>100 (0.5)	0-8V
Nguyen [5]	0.27	8.6	3085	273 (1)	0-50V
Pulskamp [6]	0.019	0.23	1060	100 (8.7)	0-20V
Mahameed [8]	0.09	0.27	200	100 (3)	0-50V
This Work	0.01	0.28	2700	317 (1)	0-30V

\* Tuning range is defined as  $(C_{max} - C_{min})/C_{min}$ , expressed as a percentage, where continuous tuning is possible between  $C_{max}$  and  $C_{min}$ .

were obtained from the measured  $S_{11}$  and evaluated using  $Q = \text{Im}(Z)/\text{Re}(Z)$ . The high  $Q$ -factors are achieved by using gold electrodes and integrating the varactor on a low loss fused silica substrate. The tuning range of the zipping varactor is very large (2700%) and this is comparable to the highest reported in the literature (3085%, [5]) for a single RF analog varactor. In addition, there is often a trade-off between  $Q$ -factor and tuning range (or tuning ratio) in high-frequency tunable varactors [15] and the  $Q$ -factor  $\times$  tuning-range figure of merit for the varactor in this work is comparable to the highest value reported previously in [5]. A comparison of the varactor in this work against others in the literature is given in Table I. Furthermore, the device footprint is very compact with an area of  $540 \times 130 \mu\text{m}^2$  which is more than ten times smaller compared to the area of the device reported in [5]. The self-resonance of the varactor is estimated to be 16.6 GHz and 87.6 GHz at the maximum and minimum capacitances, respectively. The mechanical resonance of the varactor is calculated using a finite element model to be 1.7 kHz, and hence the varactor is not likely to be adversely affected by low frequency vibrations that portable consumer electronics are exposed to.

The power handling limit of the zipping varactor has been evaluated using the method described in [16]. The effect of self-actuation due to the  $V_{dc}$ , the dc component of the RF signal is predicted using the FE model and it is observed that the tuning range of the varactor reduces to 340% (from 67 to 294 fF) when a  $V_{dc}$  of 10 V is introduced as it exceeds the initial pull-in voltage. Hence, the value of  $V_{dc}$  should not exceed approximately 9V in order to ensure negligible change in the tuning range. For a  $50 \Omega$  system, this corresponds to a maximum RF power of around 400 mW.

#### IV. CONCLUSION

A high- $Q$  RF MEMS zipping varactor with a very large tuning range has been reported in this letter. The varactor has potential applications as a tuning element in reconfigurable RF subsystems such as phase shifters, voltage-controlled oscillators, tunable filters and tunable antennas. A modified monolithic fabrication process could be used to improve the tuning characteristics of the varactor.

#### ACKNOWLEDGMENT

S.H. Pu is grateful to Kees de Groot and Nur Zatil Ismah Hashim for help with the RF measurements. The authors also thank Hong Liu for varactor cantilever height measurements.

## REFERENCES

- [1] G. M. Rebeiz, K. Entesari, I. C. Reines, S.-J. Park, M. A. El-Tanani, A. Grichener, and A. R. Brown, "Tuning in to RF MEMS," *IEEE Microw. Mag.*, vol. 10, no. 6, pp. 55–72, Oct. 2009, doi: 10.1109/MMM.2009.933592.
- [2] Z. Xiao, W. Peng, R. F. Wolffentbuttel, and K. R. Farmer, "Micromachined variable capacitors with wide tuning range," *Sens. Actuators A, Phys.*, vol. 104, no. 3, pp. 299–305, May 2003, doi: 10.1016/S0924-4247(03)00048-7.
- [3] K. F. Harsh, B. Su, W. Zhang, V. M. Bright, and Y. C. Lee, "The realization and design considerations of a flip-chip integrated MEMS tunable capacitor," *Sens. Actuators A, Phys.*, vol. 80, no. 2, pp. 108–118, Mar. 2000, doi: 10.1016/S0924-4247(99)00255-1.
- [4] R. L. Borwick, P. A. Stupar, J. F. DeNatale, R. Anderson, and R. Erlanson, "Variable MEMS capacitors implemented into RF filter systems," *IEEE Trans. Microw. Theory Techn.*, vol. 51, no. 1, pp. 315–319, Jan. 2003, doi: 10.1109/TMTT.2002.806519.
- [5] H. D. Nguyen, D. Hah, P. R. Patterson, R. Chao, W. Piyawattanametha, E. K. Lau, and M. C. Wu, "Angular vertical comb-driven tunable capacitor with high-tuning capabilities," *IEEE/ASME J. Microelectromech. Syst.*, vol. 13, no. 3, pp. 406–413, Jun. 2004, doi: 10.1109/JMEMS.2004.828741.
- [6] J. S. Pulskamp, S. S. Bedair, R. G. Polcawich, C. D. Meyer, I. Kierzewski, and B. Maack, "High- $Q$  and capacitance ratio multilayer metal-on-piezoelectric RF MEMS varactors," *IEEE Electron Device Lett.*, vol. 35, no. 8, pp. 871–873, Aug. 2014, doi: 10.1109/LED.2014.2327611.
- [7] J. Muldavin, C. Bozler, S. Rabe, and C. Keast, "Large tuning range analog and multi-bit MEMS varactors," in *IEEE MTT-S Int. Microw. Symp. Dig.*, vol. 3. Fort Worth, TX, USA, Jun. 2004, pp. 1919–1922, doi: 10.1109/MWSYM.2004.1338984.
- [8] M. Bakri-Kassem, S. Fouladi, and R. R. Mansour, "Novel high- $Q$  MEMS curled-plate variable capacitors fabricated in 0.35- $\mu\text{m}$  CMOS technology," *IEEE Trans. Microw. Theory Techn.*, vol. 56, no. 2, pp. 530–541, Feb. 2008, doi: 10.1109/TMTT.2007.914657.
- [9] R. Mahameed, M. A. El-Tanani, and G. M. Rebeiz, "A zipper RF MEMS tunable capacitor with interdigitated RF and actuation electrodes," *J. Micromech. Microeng.*, vol. 20, no. 3, p. 035014, Feb. 2010, doi: 10.1088/0960-1317/20/3/035014.
- [10] S. H. Pu, A. S. Holmes, E. M. Yeatman, C. Papavassiliou, and S. Lucyszyn, "Stable zipping RF MEMS varactors," *J. Micromech. Microeng.*, vol. 20, no. 3, p. 035030, Mar. 2010, doi: 10.1088/0960-1317/20/3/035030.
- [11] C. L. Goldsmith, A. Malczewski, Z. J. Yao, S. Chen, J. Ehmke, and D. H. Hinzel, "RF MEMS variable capacitors for tunable filters," *Int. J. RF Microw. Comput.-Aided Eng.*, vol. 9, no. 4, pp. 362–374, Jul. 1999, doi: 10.1002/(SICI)1099-047X(199907)9:4<362::AID-MMCE7>3.0.CO;2-H.
- [12] J. Reinke, G. K. Fedder, and T. Mukherjee, "CMOS-MEMS 3-bit digital capacitors with tuning ratios greater than 60:1," *IEEE Trans. Microw. Theory Techn.*, vol. 59, no. 5, pp. 1238–1248, May 2011, doi: 10.1109/TMTT.2011.2114363.
- [13] C.-Y. Lee and E. S. Kim, "Piezoelectrically actuated tunable capacitor," *IEEE/ASME J. Microelectromech. Syst.*, vol. 15, no. 4, pp. 745–755, Aug. 2006, doi: 10.1109/JMEMS.2006.878886.
- [14] D. A. Darbyshire, "Development of lead-free thin-film dielectrics for capacitor applications," Ph.D. dissertation, School Appl. Sci., Cranfield Univ., Cranfield, U.K., 2011.
- [15] M. P. J. Tiggelman, K. Reimann, F. van Rijs, J. Schmitz, and R. J. E. Huetting, "On the trade-off between quality factor and tuning ratio in tunable high-frequency capacitors," *IEEE Trans. Electron Devices*, vol. 56, no. 9, pp. 2128–2136, Sep. 2009, doi: 10.1109/TED.2009.2026391.
- [16] T. G. S. M. Rijks, P. G. Steeneken, J. T. M. van Beek, M. J. E. Uleners, A. Jourdain, H. A. C. Tilmans, J. De Coste, and R. Puers, "Microelectromechanical tunable capacitors for reconfigurable RF architectures," *J. Micromech. Microeng.*, vol. 16, no. 3, pp. 601–611, Feb. 2006, doi: 10.1088/0960-1317/16/3/016.